Published in final edited form as:
Biomaterials. 2011 September ; 32(26): 5970–5978. doi:10.1016/j.biomaterials.2011.04.059.

Determinants of the Thrombogenic Potential of Multiwalled Carbon Nanotubes

Andrew Burke[1], **Ravi Singh**[1], **David L. Carroll**[2], **John Owen**[3], **Nancy D. Kock**[4], **Ralph D'Agostino Jr**[5,7], **Frank M. Torti**[1,7], and **Suzy V. Torti**[6,7,*]

[1] Department of Cancer Biology, Wake Forest University School of Medicine, Winston Salem, NC 27157

[2] Department of Physics, Wake Forest University, Winston Salem, NC 27109

[3] Department of Medicine, Section on Hematology/Oncology, Wake Forest University School of Medicine, Winston Salem, NC 27157

[4] Department of Pathology , Wake Forest University School of Medicine, Winston Salem, NC 27157

[5] Department of Biostatistical Sciences, Wake Forest University School of Medicine, Winston Salem, NC 27157

[6] Department of Biochemistry, Wake Forest University School of Medicine, Winston Salem, NC 27157

[7] Comprehensive Cancer Center of Wake Forest University, Winston Salem, NC 27157

Abstract

Multiwalled carbon nanotubes (MWCNTs) are cylindrical tubes of graphitic carbon with unique physical and electrical properties. MWCNTs are being explored for a variety of diagnostic and therapeutic applications. Successful biomedical application of MWCNTs will require compatibility with normal circulatory components, including constituents of the hemostatic cascades. In this manuscript, we compare the thrombotic activity of MWCNTs *in vitro* and *in vivo*. We also assess the influence of functionalization of MWCNTs on thrombotic activity. *In vitro*, MWCNT activate the intrinsic pathway of coagulation as measured by activated partial thromboplastin time (aPTT) assays. Functionalization by amidation or carboxylation enhances this procoagulant activity. Mechanistic studies demonstrate that MWCNTs enhance propagation of the intrinsic pathway via a non-classical mechanism strongly dependent on factor IX. MWCNTs preferentially associate with factor IXa and may provide a platform for its activation. In addition to their effects on the coagulation cascade, MWCNTs activate platelets *in vitro*, with amidated MWCNTs exhibiting greater platelet activation than carboxylated or pristine MWCNTs. However, contrasting trends are obtained *in vivo*, where functionalization tends to diminish rather than enhance pro-coagulant activity. Thus, following systemic injection of MWCNTs in mice, pristine MWCNTs decreased platelet counts, increased vWF, and increased D-dimers. In contrast, carboxylated MWCNTS exhibited little procoagulant tendency *in vivo*, eliciting only a mild and

[*]To whom correspondence should be addressed at: Dept. Biochemistry, Wake Forest University School of Medicine, Medical Center Blvd, Winston Salem, NC 27157, Phone: 336-716-9357, Fax: 336-716-0255, storti@wfubmc.edu.

transient decrease in platelets. Amidated MWCNTs elicited no statistically significant change in platelet count. Further, neither carboxylated nor amidated MWCNTs increased vWF or D-dimers in mouse plasma. We conclude that the pro-coagulant tendencies of MWCNTs observed *in vitro* are not necessarily recapitulated *in vivo*. Further, functionalization can markedly attenuate the procoagulant activity of MWCNTs *in vivo*. This work will inform the rational development of biocompatible MWCNTs for systemic delivery.

Keywords

blood; blood compatibility; clotting; nanoparticle; platelet activation; thrombosis

1. Introduction

Carbon nanotubes (CNTs) consist of sheets of graphitic carbon formed into single-walled or multiwalled tubes (termed SWCNTs or MWCNTs, respectively). The unique combination of electrical, thermal and spectroscopic properties of these materials offers new opportunities for advances in the detection, monitoring and treatment of diseases including cancer[1]. For example, our group has shown that MWCNTs directly injected into tumors are highly effective agents for anti-tumor thermal therapy, resulting in long term remission of ~80% of tumors implanted in mice[2]. Moreover, CNTs can be taken up by cells, allowing them to act as efficient carriers of therapeutic drugs and nucleic acids[3, 4]. The ability to incorporate multiple diagnostic and therapeutic functions into a single particle makes carbon nanotubes well-suited for further biomedical development[5, 6].

The toxicity profile of MWCNTs will be a critical factor in determining their clinical utility. Examination of the toxicological profile of CNTs has largely focused on adverse effects induced by environmental exposure to CNTs, such as those created by inhalation or during manufacture. Such studies have raised concerns regarding the possibility that long (10–20 μm) CNTs induce asbestos-like reactions[7], or that inhalation of CNTs causes granulomatous pneumonia, oxidative stress, and acute inflammatory and cytokine responses[8–10]. However, many uses of CNTs as nanomedicines, including implementation as anti-cancer drugs, will necessitate systemic administration through intravenous and other routes, where alternative toxicities might be observed. Because of the well-documented ability of intravascular particulates to induce thrombosis, induction of undesired thrombotic events represents a particularly critical potential toxicity[11–14].

Many systemic components contribute to thrombosis, including coagulation factors of the intrinsic and extrinsic coagulation cascade, platelets, and endothelial cells. The effect of CNTs on some of these components has been studied. For example, pristine nanotubes without surfactant coatings have been reported to activate platelets *in vitro* and accelerate the formation of thrombi in the microvasculature of rodents following artificial induction of the hemostatic cascade[12, 13, 15–18]. However, the role of specific components of the hemostatic system, such as proteins of the coagulation cascade, as well as how MWCNTs affect the interplay among these components, remains largely unexplored. Further, CNTs used in systemic applications are almost invariably dispersed with surfactants; effects of these therapeutically relevant combinations of functionalized MWCNTs and surfactants on coagulation have not been investigated.

Typical modifications for enhanced CNT biocompatibility include covalent functionalization of the nanotube exterior with carboxyl groups (reviewed in[19]) and/or “wrapping” in long-chain surfactants (reviewed in[20]). Antibodies or other targeting moieties have also been linked to CNTs to both aid in their dispersion and promote their

accumulation in tumor tissue[21, 22]. It has been suggested that covalent functionalization can improve the overall toxicity profile of carbon nanotubes by enhancing their clearance[23]. In the present study, we assessed the potential thrombogenic effects of functionalized MWCNTs *in vitro* and *in vivo*.

2. Materials and methods

Complete experimental details are provided in *SI Materials and Methods*.

2.1. Materials

Pristine (PD15L1-5, Lot number: 40209) carboxyl (PD15L1-5-COOH, lot number: 60809) and amide-functionalized (PD15L1-5-NH_2, lot number: 60809) multiwalled carbon nanotubes were purchased from NanoLab (Waltham, MA). MWCNTs were suspended in sterile saline with 1% (wt/wt) pluronic F127 (Sigma) or DSPE-PEG (Avanti Polar Lipids) through probe tip sonication (Branson). Uncoated MWCNT suspensions were prepared using sterile saline as the solvent. All samples were autoclaved prior to use.

2.2. Platelet activation

Aliquots of PRP were incubated with increasing concentrations (10, 50 or 100 μg/mL) of either uncoated, pluronic F127 or DSPE-PEG coated MWCNTs (pristine, carboxylated or amidated) (see *Materials*) for 30 minutes at room temperature. Samples were then labeled with 20 μL of FITC-conjugated CD62P (555523) (BD Biosciences) for 15 minutes at room temperature. Platelets were then fixed in 1x formaldehyde and diluted to 1 mL final sample volume in PBS. Samples were analyzed on a FACSCaliber flow cytometer and data analyzed using CellQuest Pro software (BD Biosciences). Platelets incubated with 23 μM ADP served as the positive control while a sample fixed with 1x formaldehyde prior to ADP stimulation constituted the negative control.

2.3. Platelet aggregation

Aliquots of platelet-rich plasma were incubated with 100μg per mL pluronic F127 or DSPE-PEG_{5000} coated MWCNTs (pristine, carboxylated or amidated) (see *Materials*) for 30 minutes at room temperature. Samples were then labeled with 20 μL of FITC-conjugated CD62p (555523) (BD Biosciences) for 15 minutes at room temperature. Platelets were then fixed in formaldehyde and diluted to 1mL final sample volume in PBS. Samples were centrifuged at 800 x *g* for 15 minutes and washed with fresh PBS three times to remove plasma proteins and unbound antibody. 200 μL of washed and resuspended platelets were placed onto poly-L-lysine coated cover slips and allowed to adhere overnight at 4°C in a moistened chamber. Cover slips were then washed three times in fresh PBS and mounted on slides using 1:1 glycerol/PBS mounting medium. Platelets were imaged using an Axiovert 100M (Zeiss) confocal fluorescence microscope.

2.4. Activated partial thromboplastin time (aPTT)

Asolectin stock was prepared by homogenizing asolectin (Sigma Aldrich) at 3.8% (w/w) in physiologic saline. Asolectin was further diluted 1:35 in Owren's Veronal buffer (Dade Behring) immediately prior to use. Kaolin stock was prepared by suspending kaolin in physiologic saline at a final concentration of 20 mg/mL or 100 μg/mL.

For the aPTT assay, 50 μL of activator (either kaolin or MWCNTs) was mixed with 50 μL of diluted asolectin stock and added to 100 μL of pooled normal human plasma (PNP) (George King Biomedical) in a 300 μL reaction cup and allowed to incubate for 2 minutes. The sample was then placed in a fibrometer (BBL Fibrosystems) and activated with 100 μL

of 0.025 M calcium chloride solution. The clotting reaction was allowed to proceed to completion and the time recorded.

2.5. Nanotube binding of factor IX and factor IXa

Purified human factor IX and factor IXa (Haematologic Technologies Inc.) were individually reconstituted in TBS buffer containing 2.5 mM Ca^{2+} and 1.4 mg/mL BSA to a final concentration of 100 nM. For the experiment described in Figure S3 calcium was not added to the buffer for the samples described as “calcium-free”. The indicated nanotube preparations in either pluronic F127 or DSPE-PEG were then diluted in these solutions to final concentrations of 100 or 250 μg/mL and incubated for 1 hr at room temperature. Following incubation, samples were centrifuged at 14,000 x *g* in a Beckman microcentrifuge for 30 minutes to pellet the nanotubes and any bound protein. Control samples containing factor IX or factor IXa in buffer but no nanotubes were similarly centrifuged. Aliquots from the supernatant of each sample were withdrawn and proteins resolved by SDS-PAGE using 10% polyacrylamide gels. Gels were transferred to nitrocellulose and probed with a monoclonal mouse anti-human factor IX antibody (AHIX-5041) from Haematologic Technologies Inc. Membranes were developed by enhanced chemiluminescence method and imaged in a LAS 3000 (Fuji Medical Systems). Relative band intensities were determined using the Image J software package.

2.6. Mouse model

To establish baseline platelet counts 25 μl of blood was drawn from the tail vein by venipuncture and collected in a citrated pipette. Blood was immediately diluted in 5 ml of Isoton II buffer (Beckman Coulter) then centrifuged at 200 x *g* for 8 minutes to prepare platelet-rich plasma (PRP). 100 μl of PRP was further diluted in 10 ml of Isoton II and platelets were counted using a Beckman Coulter Z2 particle count and size analyzer.

Mice were anesthetized by isoflurane inhalation, weighed, and their tails were dipped into 50°C water to dilate the veins. A total of 250 μg of nanotubes in a 250 μl volume was administered by tail vein injection to 4–5 mice per nanotube/surfactant combination (See *Materials*). As a control, normal saline containing 1% pluronic F-127 was mixed with an equal volume of normal saline containing 1% DSPE-PEG and 250 μl of the admixture was injected into the tail vein of 4 mice. Blood was again collected from the tail vein 3 hrs, 24 hrs, and 48 hrs after nanotube injection, and platelets were counted as described above. Additionally, mice were monitored for signs of physical distress.

All mice were sacrificed 48 hrs after nanotube injection and approximately 300-500 μl of blood was collected from the inferior vena cava and placed into citrated tubes. Blood was centrifuged at 5000 x *g* in a Beckman microcentrifuge and plasma was collected and immediately frozen at −80°C for further analysis for D-dimer and mVWF.

2.7. Mouse d-dimer and vWF ELISA

Mouse plasma was diluted 1:5 in phosphate buffered saline and D-dimer (E0506Mu) or mVWF (E0833Mu) levels were quantified by ELISA using a commercial assay kit (Uscn Life Science Inc.) according to the manufacturer’s instructions.

2.8. Histology and analysis

Mice were euthanized by CO_2 asphyxiation and sections of kidney, liver, lung, heart and spleen were preserved in 10% neutral buffered formalin. The tissues were routinely processed for histology and stained with hematoxylin (HE) and phosphotungstic acid hematoxylin (PTAH). Slides were examined for evidence of MWCNT-mediated tissue damage by a board certified anatomic veterinary pathologist (NDK).

3. Results

To assess the thrombogenicity of MWCNTs, we used pristine, carboxylated or amidated MWCNTs. Carboxylated MWCNTs were selected because carboxylation is commonly used to aid in nanotube dispersion[24]; amidated MWCNTs were selected because they have peptide bonds similar to those found in targeted CNTs[25]. Each was suspended in either pluronic F127, an FDA-approved surfactant[26], or distearoylphosphoethanolamine-(polyethylene glycol)-5000 (DSPE-PEG), a modified phospholipid[27]. All nanotube preparations had similar aspect ratios, with median lengths ranging from approximately 490–580 nm, and diameters ranging from 26–31 nm as assessed by TEM (Figure S1 and Supplemental Table 1). All nanotube preparations were acidic when suspended in normal saline; however, the pH of blood did not change from its normal value of 7.4 following the addition of 100 μg/ml of any tested nanotube preparation (Supplemental Tab 1). No nanotube preparation caused hemolysis (Figure S2). Endotoxin was not detected in any nanotube preparation (Supplemental Table 1).

3.1. Effects of MWCNTs on the intrinsic clotting cascade

We first tested the ability of MWCNT preparations to activate the intrinsic coagulation cascade. We used an activated partial thromboplastin time (aPTT) assay, a standard test of coagulation factor activity that measures time to fibrin strand formation in plasma, and is used clinically to assess deficiencies in factors of the intrinsic coagulation cascade[28]. Kaolin (a negatively charged crystalline silicate) was used as a positive control. With the exception of pluronic-coated pristine MWCNTs, all nanotube preparations activated the intrinsic cascade in a dose-dependent manner, as indicated by a decrease in clotting time (Figure 1). Coating affected thrombogenicity: PEG-coated nanotubes tended to be more thrombogenic than pluronic-coated MWCNTs. For example, PEG-coated carboxylated MWCNTs were more thrombogenic than pluronic-coated carboxylated MWCNTs at all concentrations tested ($p=0.042$, $p<0.0001$ and $p<0.0001$ for 10, 50 and 100μg/mL, respectively). Functionalization also affected thrombogenicity: for example, at 100 μg/mL, PEG coated carboxylated nanotubes shortened clotting time by 41%, whereas PEG coated amidated nanotubes, shortened clotting time by 32% ($p=0.018$). Overall, carboxylated nanotubes were the most pro-thrombotic, with pluronic and PEG-coated preparations at the 100 μg/mL concentration shortening the clotting time by 33% and 41%, respectively, relative to vehicle controls ($p<0.0001$ for both).

3.2. Interaction of MWCNTs with factor IX

The intrinsic clotting cascade is a pathophysiologic thrombotic response that proceeds in a step-wise manner beginning with the activation of the apical zymogen factor XII[29]. Subsequent cleavage and activation of factor XI and factor IX leads to the formation of the tenase complex (comprised of factors X, IXa, VIIIa and Ca^{2+}). The tenase complex converges with clotting factors that are part of the extrinsic pathway initiated by vessel damage, and ultimately results in the formation of a fibrin clot (see Figure 7).

To determine which factors are required for nanotube-mediated clotting, the aPTT assay was performed in plasma selectively immuno-depleted for factors XII, XI or IX using carboxylated MWCNTs, the most pro-thrombogenic nanotube in normal plasma, to initiate clotting. Kaolin was used as a control. As anticipated, loss of any of these factors substantially lengthened coagulation time. For example, in the presence of kaolin, loss of factor XII led to a 13-fold increase in clotting time compared to normal plasma (Figure 2a) ($p<0.0001$). Consistent with the known predominant role for factor XII, the proximal factor in the pathway, in kaolin-mediated contact activation of the cascade[30], loss of factors XI and IX had significantly diminished effects on clotting time prolongation, relative to the loss

of factor XII (Figure 2a) ($p<0.001$). If MWCNTs act similarly to kaolin by serving as contact activators of factor XII, we would anticipate a spectrum of factor dependence similar to that of kaolin. Remarkably, we observed that MWCNTs exhibited a pattern of factor dependence inverse from that of kaolin: MWCNT-mediated coagulation was more sensitive to levels of factor IX than factor XII (Figure 2a). Thus, clotting times for carboxylated MWCNTs increased 4.1 and 3.6-fold in factor XII and XI deficient plasma while a 9.4-fold increase was observed with factor IX depleted plasma (Figure 2a) ($p<0.0001$).

To assess whether factor IX dependence was unique to carboxylated MWCNTs or a more general response to functionalized MWCNTs, we performed a similar analysis with amidated MWCNTs. As shown in Figure 2b, the loss of factors XII and XI lengthened nanotube-dependent clotting times by 4-fold (4.05 ± 0.66) relative to normal plasma controls, consistent with a basal requirement for these factors in normal cascade propagation (Figure 2b). Similar to our observations with carboxylated CNTs, loss of factor IX led to a greater increase in clotting times (8.99 ± 0.76 fold) than loss of either factor XII or XI. These results demonstrate a consistent difference in the coagulation response elicited by functionalized MWCNTs when compared to classical activators of the intrinsic coagulation pathway, such as kaolin (Fig. 2a). A similar preferential dependence on factor IX was observed regardless of whether MWCNTs were coated with PEG or pluronic (Figure 2b).

To confirm the dependence of nanotube-mediated coagulation on factor IX concentration, the aPTT test was performed using plasma reconstituted with a defined percentage of normal factor IX activity (see Materials and Methods). Concordant with results shown in Figure 2b, nanotube-mediated clotting times were inversely proportional to factor IX concentration (Figure 2c). Similar results were obtained using FIX-depleted plasma reconstituted with purified human FIX alone (data not shown).

Under physiologic conditions, FIXa is maximally active on the surface of activated platelets, where it becomes incorporated into the tenase complex. This conformation results in a 10^6-fold increase in FIXa activity over the unbound enzyme[31]. Thus, one possible explanation for the ability of functionalized MWCNTs to behave as factor IX-dependent enhancers of the intrinsic coagulation cascade is that they provide a physical platform for factor IXa activity. To investigate whether functionalized nanotubes bind FIXa, factors IX and IXa were separately incubated in the presence or absence of surfactant-coated nanotube preparations, and samples were centrifuged to pellet the nanotubes along with any bound protein. Incubations were performed in 165-fold molar excess of BSA to minimize non-specific binding. Aliquots of the supernatant were then gel resolved and blotted for factor IX and factor IXa. As seen in Figure 3, functionalized MWCNTs did indeed binding FIXa, depleting it from the soluble fraction. In addition, binding of factor IXa to MWCNTs exceeded that of factor IX, suggesting a preferential association of MWCNTs with factor IXa (Figure 3).

Factor IX is a member of the vitamin-K-dependent protease family (the others being factors II, VII and X) all of which have a known high affinity for calcium ions [32]. As others have already shown that the binding of some proteins to oxidized carbon nanotubes is calcium-dependent[33] we tested whether the adsorption of FIXa to functionalized nanotubes was calcium-mediated. As shown in Figure S3, the binding of FIXa to functionalized nanotube preparations in calcium-free conditions was equal to or greater than that observed when using calcium-containing buffer indicating that the binding of FIXa to nanotubes is not a calcium-dependent event. Additionally, FX (another vitamin-K-dependent protease) showed negligible binding to amidated nanotube preparations despite the marked ability of these nanotubes to adsorb FIX and FIXa (data not shown and Figure 3). This, again, suggests that the association of FIXa with functionalized nanotubes is a specific interaction.

Together, these findings are consistent with a model of functionalized nanotubes accelerating the propagation of the intrinsic clotting cascade by providing a platform for the enzymatic activity of factor IXa (see model in Figure 7).

3.3. Effect of MWCNTs on platelet activation

We next explored the effect of functionalized nanotubes on platelet activation. Platelet activation is required for efficient propagation of the clotting cascade. Activated platelets provide a phospholipid-rich surface necessary for the formation of the tenase complex and also bind and stabilize the nascent fibrin clot. Activated platelets are characterized by plasma membrane display of markers such as CD62p (an adhesion molecule also called P-selectin) as well as by aggregation state.

To determine the effect of MWCNTs on platelet activation, freshly prepared platelet-rich plasma (PRP) was incubated with pristine and functionalized MWCNTs and the platelets analyzed by flow cytometry for expression of the activation marker CD62p. Adenosine diphosphate (ADP), a well-characterized platelet agonist, served as the positive control. Consistent with previous reports[13], in the absence of a surfactant coating, MWCNTs very modestly stimulated platelet activation, with a maximal 1.8 (± 0.3)-fold increase following incubation with amide functionalized MWCNTs (Figure S4). Since MWCNTs are typically suspended in surfactants for biomedical applications, we tested whether surfactants affected the ability of MWCNTs to activate platelets. When pristine or carboxylated MWCNTs were suspended in surfactants, platelet activation remained minimal (Figure 4). However, suspension of amidated MWCNTs in pluronic F127 markedly augmented their ability to stimulate platelets (Figure 4). For example, 100 μg/mL pluronic F127-coated amidated MWCNTs increased CD62p positive platelets 29 ± 4-fold relative to untreated controls ($p<0.001$).

To ascertain whether platelet activation by amidated MWCNTs represents an independent effect of coated nanotubes on platelets or a response to coagulation factors bound to the platelet surface, freshly isolated platelets were washed and resuspended in sterile, calcium-free buffered saline to prevent the contribution of plasma factors in the activation process. Washed platelets were then incubated with pluronic F127-coated amidated MWCNTs. As before, this nanotube preparation caused a dose-dependent increase in activated platelets (Figure S5) suggesting that amidated MWCNTs directly associate with platelets and trigger activation independent of effects on clotting factors.

An additional metric of platelet activation is their ability to form aggregates. To determine if nanotube-stimulated platelets form aggregates, freshly prepared platelet-rich plasma was incubated with DSPE-PEG and pluronic F127-coated nanotubes at 100 μg/mL. Stimulated platelets were labeled with FITC-conjugated CD62p antibody and imaged by fluorescence confocal microscopy. Consistent with the previous findings, pluronic F127-coated amidated MWCNTs produced the most robust platelet aggregation; aggregated platelets expressed the activation marker CD62p (green fluorescence) (Figure 3c). Coated pristine (Figure 3c) and carboxylated nanotubes did not induce substantial aggregation.

3.4. Thrombogenicity of MWCNTs *in vivo*

These *in vitro* tests indicated that MWCNTs exhibit procoagulant effects on both proteins of the coagulation cascade and platelets. However, coagulation *in vivo* depends on multiple additional factors that can modify the overall degree of coagulopathy. Endothelial cells, for example, can release von Willebrand factor (vWF) to stimulate hemostasis[34]. Fibrinolytic pathways can also be triggered to counteract procoagulant pathways and mediate the dissolution of fibrin clots. To assess the net effect of MWCNTs on these multiple

interconnected pathways, we next tested MWCNTs for procoagulant activity *in vivo*. Mice were injected intravenously with 250 μg of three different types of MWCNTs (pristine, carboxylated, and amidated MWCNTs), each suspended in two different coatings (normal saline containing 1% pluronic F127, or 1% DSPE-PEG). This dose was selected to approximate the 100 μg/ml dose used in our *in vitro* assays. Control mice were injected with vehicle alone. Blood was collected over 48 hrs, and tissues were harvested and analyzed at the final timepoint.

Injection of 250 μg of pristine MWCNTs proved acutely lethal, independent of the coating, and all mice died or required humane euthanasia within 15 minutes to a few hours after nanotube administration. Complete necropsy with histology showed that blockade of the pulmonary vasculature with ensuing respiratory and possibly cardiac distress was the most likely cause of death in these mice. In contrast, injection of 250 μg of either amidated MWCNTs or carboxylated MWCNTs was well tolerated.

To assess effects of amidated MWCNTs and carboxylated MWCNTs on coagulation, we first measured the number of circulating platelets. In all cases, a transient drop in platelet count was observed at the 3 hr time point, followed by a rebound to pre-injection levels at 24 and 48 hrs (Figure 5a). The decline at 3 hrs ranged from a 10% drop in platelets in the control group injected with saline (likely due to the increase in blood volume following injection) to a maximal drop of approximately 50% for the group injected with carboxylated MWCNTs in pluronic F127. When compared to control, the only statistically significant decrease in platelets at 3 hrs was observed in mice injected with carboxylated MWCNTs in pluronic F127 ($p=.0004$). Overall, statistical analysis of platelet counts across all time points indicated that only treatment with carboxylated MWCNTs in pluronic F127 resulted in a drop in platelet counts that was significantly different from controls ($p=0.0019$). This was strikingly different from amidated MWCNT treatment, for example, which was indistinguishable from control in its effect on platelet count *in vivo* ($p=0.79$).

We also assessed effects of injection of functionalized MWCNTs on levels of murine vWF (mVWF) and D-dimer in the blood. vWF is released following endothelial cell damage, and can trigger coagulation[35]. D-dimers are produced by degradation of cross-linked fibrin, and are used in the clinical assessment of hypercoagulable states[36]. No significant difference in murine D-dimer and mVWF levels were detected between the carboxylated or amidated MWCNT-treated and control animals (Figure 5b).

We also performed histologic examination of the lung, liver, spleen, heart, and kidney to search for evidence of fibrin clots. As a positive control, mice were injected with collagen and epinephrine to induce intravascular coagulation[37]. Tissue sections were examined in a blinded fashion by a board certified anatomic veterinary pathologist (NDK); representative lung sections are shown in Figure 6 and of remaining tissues in Figures S6-9. Although small intravascular aggregates of carboxylated and amidated nanotubes could be detected in the lungs, there was no evidence of thrombus formation in mice injected with these MWCNTs in any tissue examined. Thrombi were readily detectable in the collagen/epinephrine positive control (Figure 6).

Since a high dose of pristine nanotubes proved lethal, we injected mice with a lower dose (125 μg) of pristine nanotubes to assess their effects on coagulation *in vivo*. All mice treated with pristine nanotubes exhibited signs of distress (difficulty breathing, hunched posture, and isolation/immobility) by 48 hrs after injection. Further, unlike the carboxylated and amidated MWCNT-treated mice, significant drops in platelet levels were noted for the duration of the study in mice treated with pristine MWCNTs coated in either PEG or pluronic (Figure 5c) ($p<0.001$ versus control), and elevated D-dimer and mVWF levels were

detected (Figure 5d). Histologic examination revealed abundant intravascular aggregates of nanotubes in the lungs and kidneys, particularly in mice injected with pristine MWCNTs suspended in pluronic; however, thrombi were not detected.

4. Discussion

Our work identifies potential procoagulant activities of MWCNTs that should be evaluated as future applications of these materials are pursued (Figure 7). In particular, we observed that functionalized MWCNTs can stimulate thrombosis through three independent mechanisms: a mechanism involving factor IX (Figure 2); a classical mechanism involving factor XII (Figure 1); and a factor-independent mechanism involving activation of platelets (Figure 4). Mechanistically, stimulation of the intrinsic coagulation cascade by MWCNTs may occur through their ability to bind factor IXa and provide a platform that enhances its enzymatic activity (Figure 3).

Both *in vitro* and *in vivo*, effects of functionalization by carboxylation or amidation generally dominated effects of coating on the procoagulant activity of MWCNTs. All functionalized MWCNTs wrapped in pluronic F127 activated the intrinsic coagulation cascade (Figure 1). Since poloxamers similar to pluronic F127 are believed to be rapidly displaced by plasma proteins following systemic delivery[38], we tested whether MWCNTs cloaked in DSPE-PEG, a more stable coating[27], would be prevented from triggering this response. However, coating with DSPE-PEG did not mitigate but rather tended to exacerbate the pro-coagulant activity of MWCNTs *in vitro* (Figure 1).

Covalent functionalization similarly proved much more critical than coating in determining the prothrombogenic activity of MWCNTs *in vivo*. However, contrary to what we had observed *in vitro*, we found that pristine MWCNTs were substantially more toxic following intravenous injection in mice than functionalized nanotubes. When injected at a dose of 250 μg, pristine MWCNT were acutely lethal, inducing blockage of the pulmonary vasculature. In contrast, an equivalent dose of covalently functionalized MWCNTs exerted only a modest effect on coagulation *in vivo*, with their sole measurable effect being a transient depletion of platelets, an effect that was also independent of coating (Figure 5). Even when injected at a two-fold lower dose (125 μg), pristine MWCNTs were substantially more thrombogenic than functionalized MWCNT and induced significantly elevated vWF and D-dimer levels, independent of whether they were coated in pluronic F127 or DSPE-PEG (Figure 5).

One explanation for the apparent contradictory behavior of pristine MWCNTs *in vitro* and *in vivo* may be found in the histology of mice following intravenous administration. Unlike what was observed in mice receiving carboxylated or amidated MWCNTs, pristine nanotubes formed large, intravascular aggregates in the lungs (Figure 6) as well as in other tissues (Supplemental Figures 6–9). These aggregates may have caused direct, physical damage to the local vascular endothelium which would be an initiating event for the extrinsic clotting cascade. Activation of the extrinsic cascade would account for the rise in both vWF and D-dimer levels observed in mice following administration of the pristine MWCNTs (Figure 5). This potential ability to activate the extrinsic cascade would not have been detected by our *in vitro* assays (which assessed the intrinsic cascade) and would only become apparent in the *in vivo* setting. This further serves to emphasize the importance of animal studies to complement *in vitro* findings.

Given the continuous, dynamic interaction between pro- and anticoagulant pathways involved in the maintenance of normal hemostasis[35], homeostatic mechanisms may also contribute to counteracting procoagulant activities of MWCNTs *in vivo*, and may explain why amidated MWCNTs, as noted, exhibited very little pro-coagulant activity *in vivo*

(Figure 5), despite an ability to activate both the intrinsic coagulation cascade (Figure 1) and platelets (Figure 4) *in vitro*. We also note that effects we observed were dose-dependent, and that our *in vivo* studies deliberately used doses at or near the tolerable limit. Many applications, especially use of targeted nanotubes, will likely require substantially less material, which can also be expected to reduce pro-coagulant activity *in vivo.*

5. Conclusions

Our results demonstrate that MWCNTs have thrombogenic potential that can be substantially moderated through covalent functionalization. The systemic administration of covalently functionalized MWCNTs does not initiate a strongly pro-coagulant state, despite the ability of MWCNTs to activate coagulation proteins and platelets *in vitro*. The ability to control the pro-coagulant tendencies of MWCNTs through functionalization may be an important factor in their ultimate clinical use.

Supplementary Material

Refer to Web version on PubMed Central for supplementary material.

Acknowledgments

We are grateful to Dr. Roy Hantgan for advice and assistance in the collection and analysis of platelets and to Ken Grant and the Comprehensive Cancer Center Microscopy Core for assistance with confocal and electron microscopy. We thank Caryl Adams, Diane Meares and Heather Lawson of the Special Hematology Lab for their assistance in blood collection and Heather Hatcher and Charlotte Williams for aid in digital photography. This work was supported in part by grants RO1CA12842 from the National Institutes of Health (SVT) and Department of Defense Breast Cancer Research Program Predoctoral Traineeship Award BC093336 (AB). R.S. was supported in part by training grant T32CA079448 and by National Institutes of Health grant K99CA154006.

References

1. Kostarelos K, Bianco A, Prato M. Promises, facts and challenges for carbon nanotubes in imaging and therapeutics. Nat Nanotechnol. 2009; 410:627–633. [PubMed: 19809452]
2. Burke A, Ding XF, Singh R, Kraft RA, Levi-Polyachenko N, Rylander MN, et al. Long-term survival following a single treatment of kidney tumors with multiwalled carbon nanotubes and near-infrared radiation. Proc Natl Acad Sci U S A. 2009; 10631:12897–12902. [PubMed: 19620717]
3. Raffa V, Ciofani G, Nitodas S, Karachalios T, D'Alessandro D, Masini M, et al. Can the properties of carbon nanotubes influence their internalization by living cells? Carbon. 2008; 4612:1600–1610.
4. Singh R, Pantarotto D, McCarthy D, Chaloin O, Hoebeke J, Partidos CD, et al. Binding and condensation of plasmid DNA onto functionalized carbon nanotubes: toward the construction of nanotube-based gene delivery vectors. J Am Chem Soc. 2005; 12712:4388–4396. [PubMed: 15783221]
5. Donglu S. Integrated multifunctional nanosystems for medical diagnosis and treatment. Adv Funct Mater. 2009; 1921:3356–3373.
6. Klingeler R, Hampel S, Buchner B. Carbon nanotube based biomedical agents for heating, temperature sensoring and drug delivery. Int J Hypertherm. 2008; 246:496–505.
7. Schipper ML, Nakayama-Ratchford N, Davis CR, Kam NWS, Chu P, Liu Z, et al. A pilot toxicology study of single-walled carbon nanotubes in a small sample of mice. Nat Nanotechnol. 2008; 34:216–221. [PubMed: 18654506]
8. Shvedova AA, Kisin ER, Mercer R, Murray AR, Johnson VJ, Potapovich AI, et al. Unusual inflammatory and fibrogenic pulmonary responses to single-walled carbon nanotubes in mice. Am J Physiol-Lung C. 2005; 2895:L698–L708.
9. Park EJ, Cho WS, Jeong J, Yi J, Choi K, Park K. Pro-inflammatory and potential allergic responses resulting from B cell activation in mice treated with multi-walled carbon nanotubes by intratracheal instillation. Toxicology. 2009; 2593:113–121. [PubMed: 19428951]

10. Ryman-Rasmussen JP, Cesta MF, Brody AR, Shipley-Phillips JK, Everitt JI, Tewksbury EW, et al. Inhaled carbon nanotubes reach the subpleural tissue in mice. Nat Nanotechnol. 2009; 411:747–751. [PubMed: 19893520]
11. Mayer A, Vadon M, Rinner B, Novak A, Wintersteiger R, Fröhlich E. The role of nanoparticle size in hemocompatibility. Toxicology. 2009; 2582–3:139–147.
12. Radomski A, Jurasz P, Alonso-Escolano D, Drews M, Morandi M, Malinski T, et al. Nanoparticle-induced platelet aggregation and vascular thrombosis. Br J Pharmacol. 2005; 1466:882–893. [PubMed: 16158070]
13. Semberova J, De Paoli Lacerda SH, Simakova O, Holada K, Gelderman MP, Simak J. Carbon nanotubes activate blood platelets by inducing extracellular Ca2+ influx sensitive to calcium entry inhibitors. Nano Lett. 2009; 99:3312–3317. [PubMed: 19736974]
14. Dobrovolskaia MA, Aggarwal P, Hall JB, McNeil SE. Preclinical studies to understand nanoparticle interaction with the immune system and its potential effects on nanoparticle biodistribution. Mol Pharm. 2008; 54:487–495. [PubMed: 18510338]
15. Deng XY, Wu F, Liu Z, Luo M, Li L, Ni QS, et al. The splenic toxicity of water soluble multi-walled carbon nanotubes in mice. Carbon. 2009; 476:1421–1428.
16. Qu GB, Bai YH, Zhang Y, Jia Q, Zhang WD, Yan B. The effect of multiwalled carbon nanotube agglomeration on their accumulation in and damage to organs in mice. Carbon. 2009; 478:2060–2069.
17. Yang ST, Wang X, Jia G, Gu YQ, Wang TC, Nie HY, et al. Long-term accumulation and low toxicity of single-walled carbon nanotubes in intravenously exposed mice. Toxicol Lett. 2008; 1813:182–189. [PubMed: 18760340]
18. Bihari P, Holzer M, Praetner M, Fent J, Lerchenberger M, Reichel CA, et al. Single-walled carbon nanotubes activate platelets and accelerate thrombus formation in the microcirculation. Toxicology. 2010; 2692–3:148–154.
19. Tasis D, Tagmatarchis N, Georgakilas V, Prato M. Soluble carbon nanotubes. Chem- Eur J. 2003; 917:4001–4008.
20. Nakashima N, Fujigaya T. Fundamentals and applications of soluble carbon nanotubes. Chem Lett. 2007; 366:692–697.
21. Liu Z, Cai WB, He LN, Nakayama N, Chen K, Sun XM, et al. In vivo biodistribution and highly efficient tumour targeting of carbon nanotubes in mice. Nat Nanotechnol. 2007; 21:47–52. [PubMed: 18654207]
22. McDevitt MR, Chattopadhyay D, Kappel BJ, Jaggi JS, Schiffman SR, Antczak C, et al. Tumor targeting with antibody-functionalized, radiolabeled carbon nanotubes. J of Nucl Med. 2007; 487:1180–1189. [PubMed: 17607040]
23. Lacerda L, Ali-Boucettal H, Herrero MA, Pastorin G, Bianco A, Prato M, et al. Tissue histology and physiology following intravenous administration of different types of functionalized multiwalled carbon nanotubes. Nanomedicine. 2008; 32:149–161. [PubMed: 18373422]
24. Zhang Y, Bai YH, Yan B. Functionalized carbon nanotubes for potential medicinal applications. Drug Discov Today. 2010; 1511–12:428–435.
25. Sun YP, Fu KF, Lin Y, Huang WJ. Functionalized carbon nanotubes: properties and applications. Accounts Chem Res. 2002; 3512:1096–1104.
26. Arutyunyan NR, Baklashev DV, Obraztsova ED. Suspensions of single-wall carbon nanotubes stabilized by pluronic for biomedical applications. Eur Phys J B. 2010; 752:163–166.
27. Prencipe G, Tabakman SM, Welsher K, Liu Z, Goodwin AP, Zhang L, et al. PEG branched polymer for functionalization of nanomaterials with ultralong blood circulation. J Am Chem Soc. 2009; 13113:4783–4787. [PubMed: 19173646]
28. Matchett MO, Ingram GI. Partial thromboplastin time test with kaolin. Normal range and modifications for the diagnosis of haemophilia and Christmas disease. J Clin Pathol. 1965; 18:465–471. [PubMed: 14318702]
29. Colman RW. Surface-mediated defense reactions - the plasma contact activation system. J Clin Invest. 1984; 735:1249–1253. [PubMed: 6371055]

30. Citarella F, te Velthuis H, Helmer-Citterich M, Hack CE. Identification of a putative binding site for negatively charged surfaces in the fibronectin type II domain of human factor XII - an immunochemical and homology modeling approach. Thromb and Haemos. 2000; 846:1057–1065.

31. Duffy EJ, Lollar P. Intrinsic pathway activation of factor X and its activation peptide-deficient derivative, factor Xdes-143–191. J Biol Chem. 1992; 26711:7821–7827. [PubMed: 1560014]

32. Sunnerhagen M, Drakenberg T, Forsen S, Stenflo J. Effect of Ca2+ on the structure of vitamin K-dependent coagulation factors. Haemostasis. 1996; 26 (Suppl 1):45–53. [PubMed: 8904173]

33. Salvador-Morales C, Townsend P, Flahaut E, Venien-Bryan C, Vlandas A, Green MLH, et al. Binding of pulmonary surfactant proteins to carbon nanotubes; potential for damage to lung immune defense mechanisms. Carbon. 2007; 453:607–617.

34. Blann AD. Plasma von willebrand factor, thrombosis, and the endothelium: the first 30 years. Thromb Haemos. 2006; 951:49–55.

35. Arnout J, Hoylaerts MF, Lijnen HR. Haemostasis. Handb Exp Pharmacol. 2006; 176(Pt 2):1–41. [PubMed: 17001771]

36. Manetti L, Bogazzi F, Giovannetti C, Raffaelli V, Genovesi M, Pellegrini G, et al. Changes of coagulation indexes and occurrence of venous thromboembolism in patients with Cushing's syndrome: results from a prospective study before and after surgery. Eur J Endocrinol. 2010 Epub ahead of print.

37. DiMinno G, Silver MJ. Mouse antithrombotic assay: a simple method for the evaluation of antithrombotic agents in vivo. Potentiation of antithrombotic activity by ethyl alcohol. J Pharmacol Exp Ther. 1983; 2251:57–60. [PubMed: 6834277]

38. Cherukuri P, Gannon CJ, Leeuw TK, Schmidt HK, Smalley RE, Curley SA, et al. Mammalian pharmacokinetics of carbon nanotubes using intrinsic near-infrared fluorescence. Proc Natl Acad Sci U S A. 2006; 10350:18882–18886. [PubMed: 17135351]

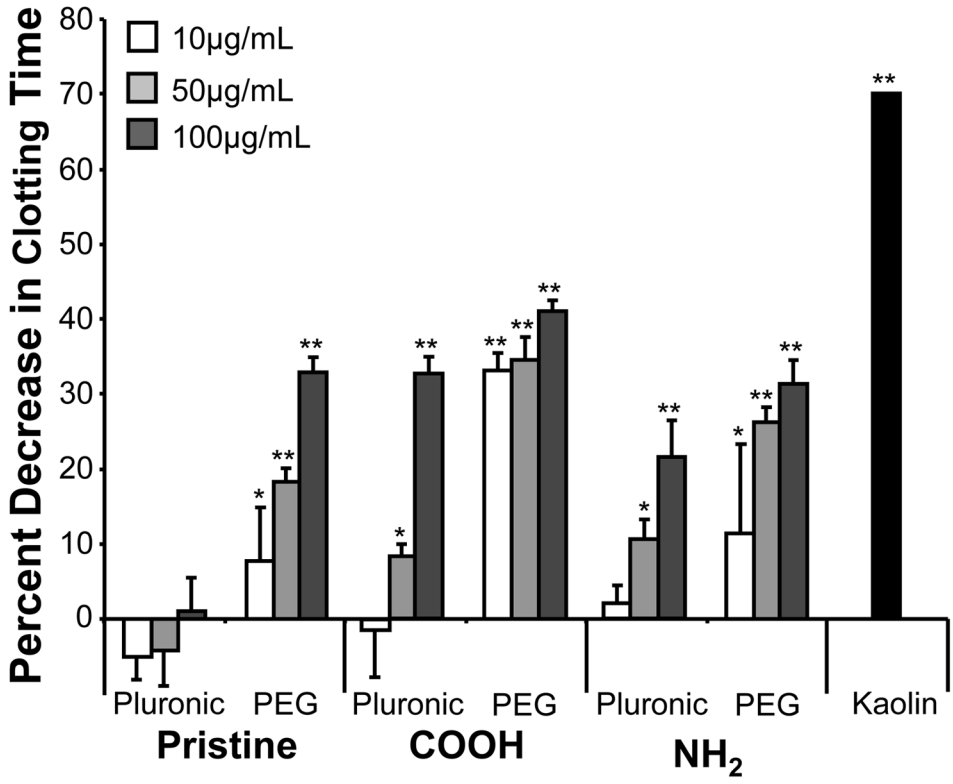

Figure 1. MWCNTs activate the intrinsic coagulation cascade

Activation status of the intrinsic clotting cascade (ICC) was monitored by the activated partial thromboplastin time (aPTT) assay. Pristine, carboxylated and amidated MWCNTs suspended in either pluronic or DSPE-PEG were tested at the indicated concentrations in pooled normal plasma (PNP). Kaolin served as the positive control. Graphed are mean decreases in time to clot formation (± s.d.) normalized to the respective vehicle controls. * $p<0.02$, ** $p<0.0005$ relative to vehicle controls.

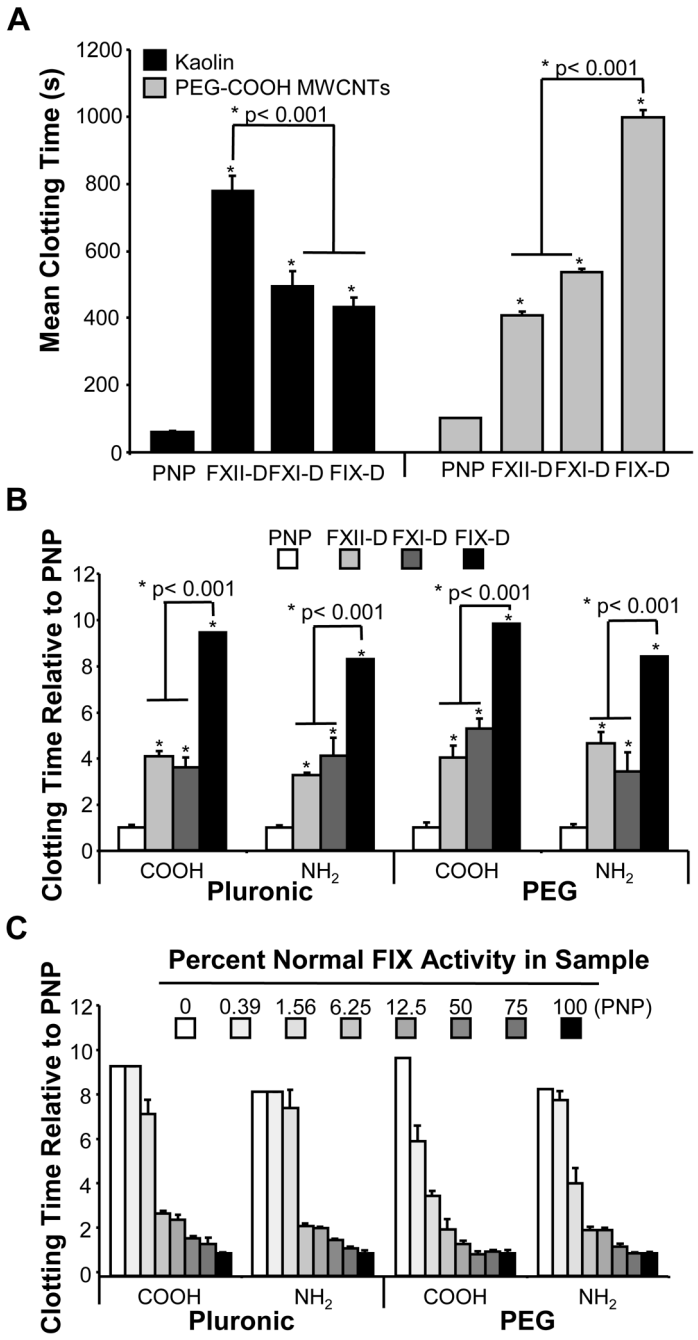

Figure 2. MWCNTs are non-classical activators of the intrinsic clotting cascade with a novel dependence on FIX

a, The thrombogenic potential of PEG-coated carboxylated MWCNTs was compared to kaolin (the prototypical ICC activator) at an identical concentration of 100 μg/mL by aPTT using either pooled normal plasma or plasma selectively immuno-depleted for the indicated clotting factors. Graphed are mean clotting times (± s.d.). (*p<0.0001). In response to kaolin, factor XII deficiency prolonged clotting time to a greater extent than deficiency of either factors XI or IX (*p<0.0001). Conversely, clotting times were prolonged to a greater extent in plasma depleted for factor IX than in plasma depleted for either factor XII or XI (*p<0.0001) in response to MWCNT stimulation. **b,** Relative clotting times for MWCNTs

(100 μg/mL) in PNP or plasma selectively immuno-depleted for the indicated clotting factors as determined by aPTT. Clotting time of PNP was set at 1.0. *p<0.001 relative to PNP. **c,** Relative clotting times for functionalized MWCNTs in plasma containing a defined percentage of normal FIX activity. Clotting time of PNP (defined as 100% FIX activity) was set at 1.0. Graphed are means and standard deviations (n=3).

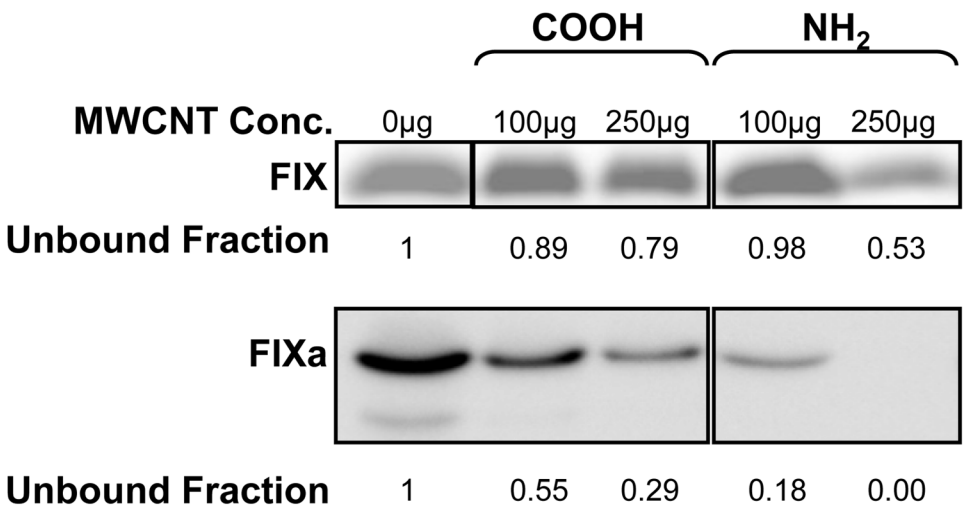

Figure 3. MWCNTs preferentially bind FIXa

Purified FIX and FIXa at 100 nM were incubated with pluronic F127-coated carboxylated MWCNT and amidated MWCNT suspensions at either 100 or 250 μg/mL in TBS buffer containing 2.5 mM calcium and a 165-fold excess of bovine serum albumin (BSA). Following 30 minutes of incubation nanotubes with bound proteins were pelleted by centrifugation and aliquots of the supernatant analyzed by Western blot for FIX and FIXa protein levels. Band intensities were quantified and normalized to their respective controls (0 μg MWCNT). Shown is a representative blot of 3 independent experiments.

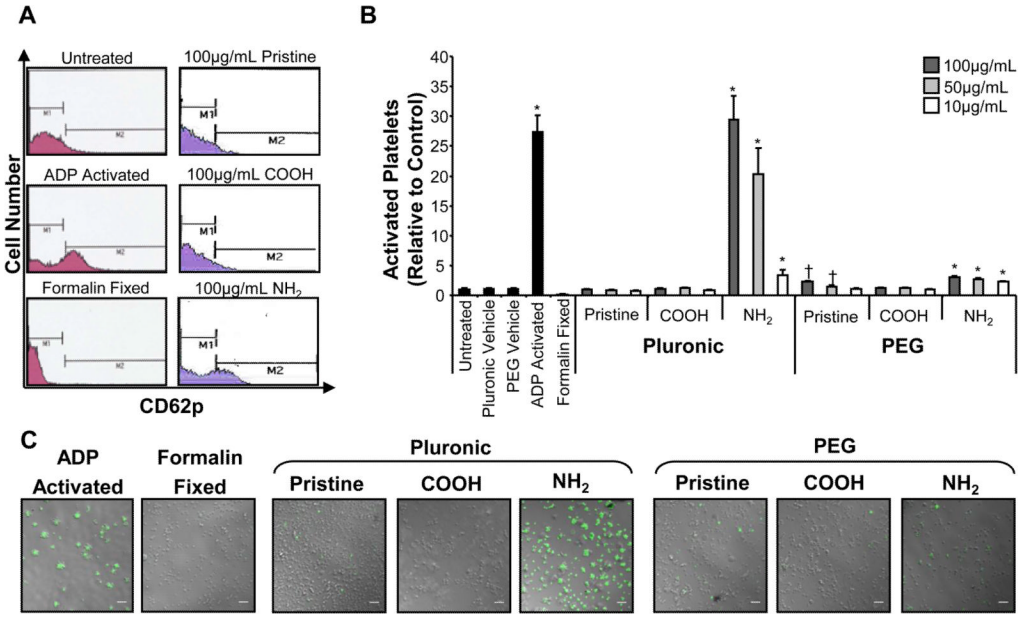

Figure 4. MWCNTs differentially activate platelets and induce their aggregation

a, Representative histograms of control and 100 μg/mL pluronic F127-coated pristine, carboxylated, and amidated MWCNT treatment conditions. M1 gate delineates the "resting" platelet population; M2 the "activated" population. **b**, Platelet rich plasma was incubated with MWCNT suspensions at the indicated final concentrations for 30 minutes prior to fixation and labeling with a FITC-conjugated CD62p antibody. The relative number of activated platelets was determined by flow cytometry. The percent activated platelets in untreated samples was set at 1.0, and the ratio of activated platelets in control vs MWCNT-treated samples was calculated. Graphed are means and standard deviations (n=3). *$p<0.005$, † $p<0.02$ relative to vehicle control **c**, Platelet rich plasma was incubated with MWCNT suspensions at 100 μg/mL for 30 minutes prior to being formalin fixed and labeled with a FITC-conjugated CD62p antibody. Platelets were washed and placed on poly-L lysine coated coverslips which were mounted and imaged by confocal microscopy. Green fluorescence denotes CD62p expression. Scale bar represents 10 μm.

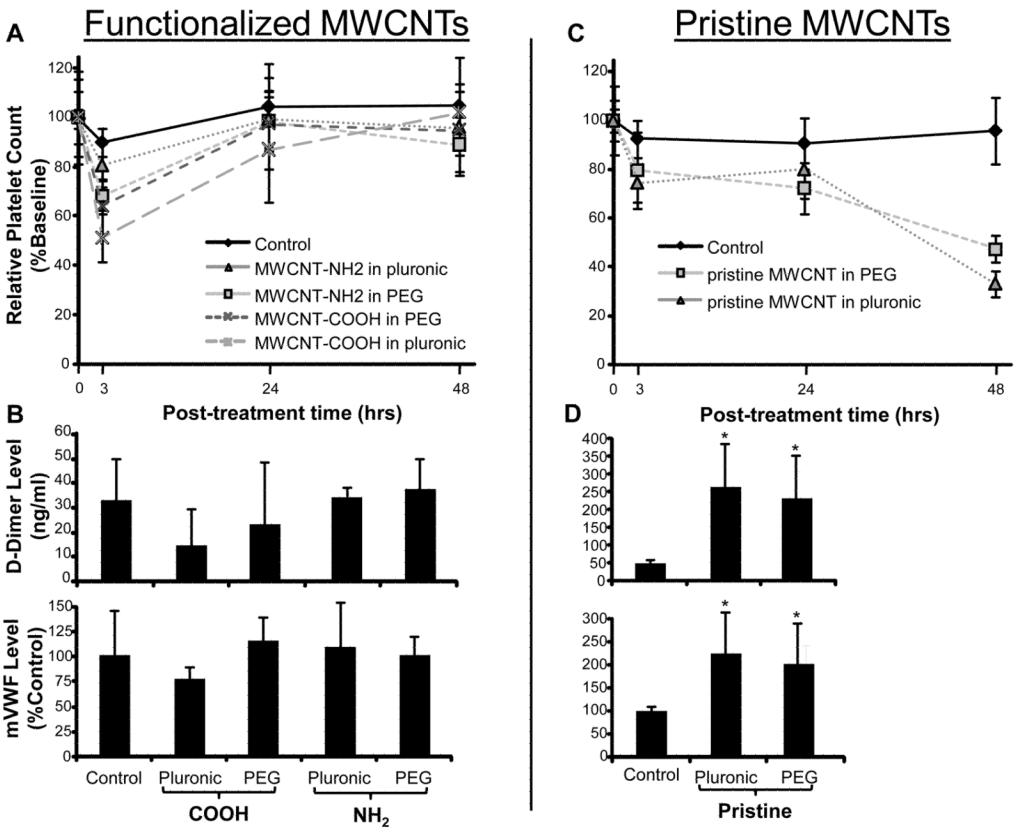

Figure 5. Thrombogenic activity of MWCNTs *in vivo*

Mice were intravenously injected with 250 μg of carboxylated (COOH) or amidated (NH2) MWCNT (**a, b**) or 125 μg of pristine MWCNT (**c, d**) in 1% pluronic F127 or 1% DSPE-PEG (w/vol) in normal saline. Circulating platelet levels were determined over time (**a, c**) and normalized to baseline platelet count (100%). Plasma D-dimer and mVWF levels were determine by ELISA 48 hrs after nanotube administration (**b, d**). mVWF levels are presented as relative to levels measured in mock treated control animals (100%). Data are presented as the mean of at least 4 samples (± s.d.). *p<0.02 versus control.

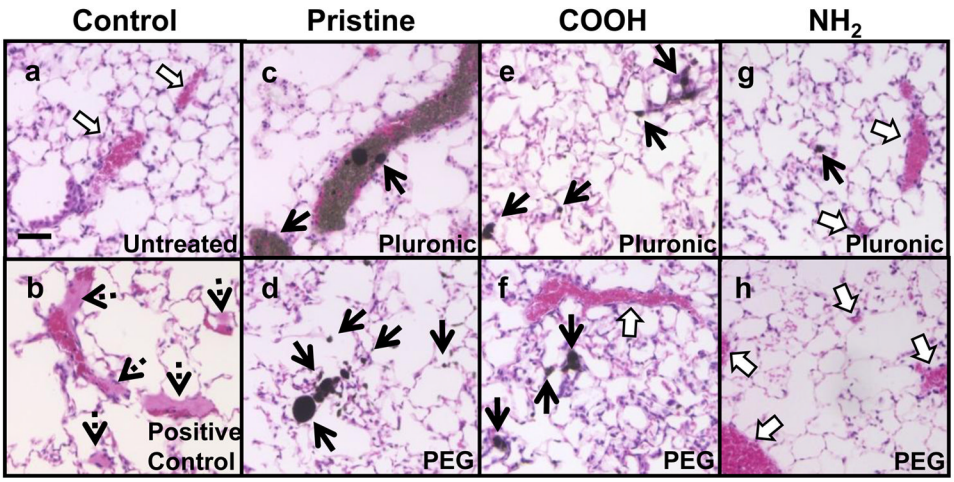

Figure 6. Photomicrographs of mouse lungs following IV injection of 250 μg MWCNTs

Tissue sections were examined for evidence of intravascular MWCNT accumulation and coagulation. White arrows show vessels filled with normal blood cells, dashed black arrows indicate intravascular coagulated blood (thrombi), and black arrows show black pigmented intravascular accumulations of MWCNTs. Representative sections are shown from mice treated as follows: **a**. Untreated control; **b**. Positive control treated with collagen and epinephrine to induce coagulation; **c, e, g**. Pristine, carboxylated, and amidated MWCNT respectively in 1% pluronic F127; **d, f, h**. Pristine, carboxylated, and amidated MWCNT respectively in 1% DSPE-PEG. Due to the acute toxicity of pristine MWCNTs, sections were prepared 15 min after injection in **c** and after 16 hrs in **d**. All others represent 48 hrs after injection. Bar equals 100 μm.

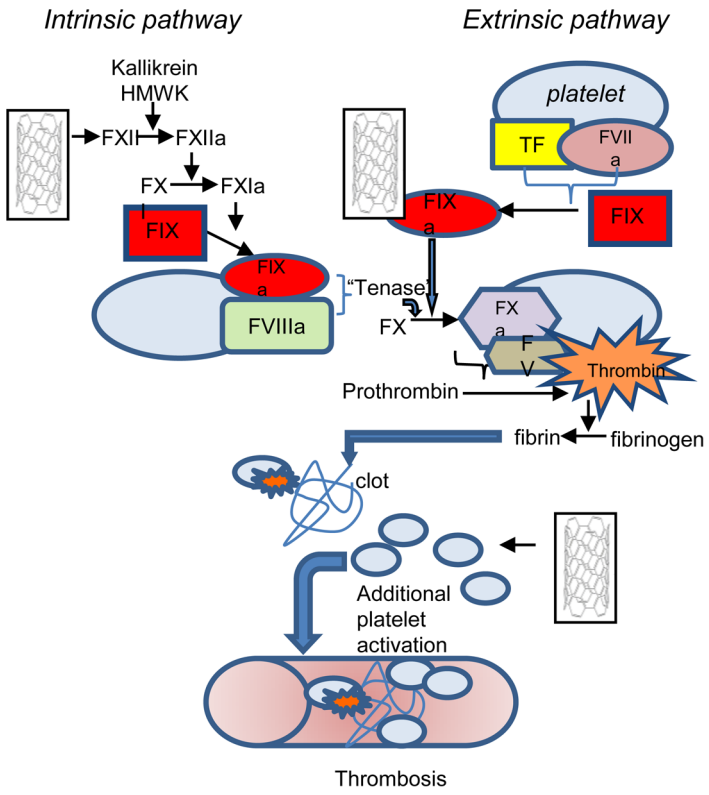

Figure 7. Model of MWCNT-mediated thrombosis

MWCNT can stimulate thrombosis through three independent mechanisms: activation of factor XII, binding of factor IXa, and activation of platelets. Nanotube association with FIXa appears to be more important than FXII in nanotube-mediated activation of the intrinsic pathway.